Real-Time Deformability Cytometry as a Label-Free Indicator of Cell Function*

O. Otto, P. Rosendahl, S. Golfier, A. Mietke, M. Herbig, A. Jacobi, N. Töpfner, C. Herold, D. Klaue, S. Girardo, M. Winzi, E. Fischer-Friedrich, and J. Guck

Abstract— **The mechanical properties of cells are known to be a label-free, inherent marker of biological function in health and disease. Wide-spread utilization has so far been impeded by the lack of a convenient measurement technique with sufficient throughput. To address this unmet need, we have recently introduced real-time deformability cytometry (RT-DC) for continuous mechanical single-cell classification of heterogeneous cell populations at rates of several hundred cells per second. Cells are driven through the constriction zone of a microfluidic chip leading to cell deformations due to hydrodynamic stresses only. Our custom-built image processing software performs image acquisition, image analysis and data storage on the fly. The ensuing deformations can be quantified and an analytical model enables the derivation of cell material properties. Performing RT-DC we highlight its potential to identify rare objects in heterogeneous suspensions and to track drug-induced changes in cells. In summary, RT-DC enables marker-free, quantitative phenotyping of heterogeneous cell populations with a throughput comparable to standard flow cytometry.**

I. Introduction

The mechanical properties of cells have been of scientific interest for almost 150 years [1,2]. This fascination is obvious considering that cell mechanics is directly being linked to cell function through the cytoskeleton, which is the main determinant of the deformability of single animal cells [3,4]. Any cellular process that requires the activity of the cytoskeleton, such as migration, mitosis or phagocytosis, can be investigated by tracking changes in the deformability of the entire cell [5]. This shows the power of using mechanical phenotyping as a non-invasive and label-free way of quantifying functional changes of physiological but also pathological origin. Its biological relevance has already been proven in research on cell differentiation [6-9] and malignant transformation [10-16] and led to the development of many basic research methods like micropipette aspiration, atomic force microscopy and optical stretching [17,18].

Techniques investigating cell mechanics generally have throughput rates of 10 – 100 cells/h, which is too slow for applications where large quantities of cells need to be studied. High numbers are relevant for example in screening procedures where only a small sub-fraction of cells in a heterogeneous population is of interest. As such, the promise of wide-spread application of mechanical phenotyping in biology, biotechnology and medicine has so far been hampered by the lack of a suitable, robust and operator-friendly method with sufficient throughput that can be used in a similar way as flow cytometry.

A recent development utilizes hydrodynamic cell stretching to address this need. In general, the hydrodynamic interaction with the flow of the surrounding medium causes stress on the surface of a cell and a subsequent deformation. One important approach operating in an inertia-dominated regime is deformability cytometry (DC) [19]. While cells are decelerated at the stagnation point of a fast extensional flow the resulting deformation is recorded with a high-speed camera operating at 100,000 fps. Due to the massive amount of data acquired, the image analysis of a two seconds long experiment takes 15 - 20 minutes and has to be performed offline after the experiment has finished. DC enables measurement rates on the order of 1,000 cells/s and, thus, fulfills one important translational requirement of mechanical phenotyping. In this context, the application of DC for the diagnostic analysis of pleural effusions was already shown [16]. However, the very high velocities required, and inertial forces generated, also fluidize the cell and render the method mostly insensitive to cytoskeletal changes [19], which limits the range of applications.

Here, we report the characterization and first measurements using real-time deformability cytometry (RT-DC), a method that had recently been introduced [20]. It allows for real-time measurement of shear stress-induced cell deformation at throughput rates in excess of 100 cells/s. RT-DC has the potential to be applied in diverse fields of life-sciences, biotechnology and medicine, where a label-free characterization of cell function is required.

II. Material and Methods

Cells

HL60 cells are a myeloid precursor cell line, which was originally derived from a patient suffering from acute promyelocytic leukemia (APL). It has been modified to the current HL60/S4 line (gift from Donald and Ada Olins, Department of Pharmaceutical Sciences, College of Pharmacy, University of New England) used in this work. Cells are cultured in RPMI-1640 medium (Life Technologies) with 10% heat-inactivated fetal calf serum (Life Technologies) and 1% penicillin / streptomyocin (Life Technologies) in a Hera Cell standard incubator (Life Technologies). As culture conditions 37°C, 5% CO2 and 95% air have been used.

*Research supported by the Alexander von Humboldt Foundation.

Biotechnology Center, Technische Universität Dresden, 01307 Dresden, Germany (e-mail: jochen.guck@tu-dresden.de).

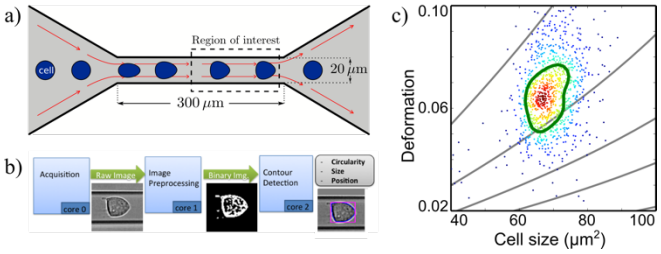

Figure 1: Real-time deformability cytometry setup. a) Sketch of microfluidic chip geometry showing a suspended cell approaching the 300 µm long channel with a 20 µm x 20 µm squared cross-section. The cell is deformed by hydrodynamic interaction only. Image acquisition is carried out at the rear part of the channel and integrates b) image preprocessing including background subtraction and thresholding as well as contour detection and quantification of circularity, size and position. c) RT-DC plot showing Deformation = 1 – circularity vs. cell size for an exemplary measurement of N=1,118 cells. Curved iso-elasticity lines indicate lines of equal mechanical properties while the density of events is color-coded. Green line represents 50% of the maximum density.

DMSO assay

HL60 cells have been treated with 10% dimethylsulfoxide (DMSO, Sigma Aldrich), which is an amphipathic molecule being used e.g. as a cryoprotectant and a vehicle in drug delivery [21]. It is known to penetrate cell membranes and causes harmful ruptures at higher concentrations thus inducing apoptosis / necrosis [22-24]. After an incubation time of 10 minutes, the cells are washed in ice-cold phosphate saline buffer (PBS- without Mg^{2+} and Ca^{2+}) using an Eppendorf centrifuge at 115 g for 5 minutes (Eppendorf 8505 R, Eppendorf) and re-suspended in PBS- and 0.5% (w/v) methylcellulose (Sigma Aldrich) which is used as the experimental medium (MC-PBS). Methylcellulose increases the density of PBS- and reduces the sedimentation of cells during an experiment.

RT-DC experimental protocol

RT-DC experiments are carried out at a cell concentration of > 10^6 cells per ml and require a minimal absolute sample volume of 100 µl. Re-suspended cells are drawn into a 1 ml syringe and connected to polymer tubing, which has been cleaned using 70% ethanol and 200 nm sterile-filtered (Sigma Aldrich) de-ionized water. After connecting tubing for cells, sheath fluid and outlet to the syringe pump and microfluidic chip a flow is stabilized for 1 minute at a constant flow rate. In a typical experiment a flow rate of 0.04 µl/s is applied and several thousand cells are analyzed.

III. Results and Discussion

Experimental Setup

The experimental realization of real-time deformability cytometry (RT-DC) is described elsewhere [20]. Briefly, the setup consists of a microfluidic chip made of polydimethylsiloxane in a soft-lithography process. The chip is assembled on a standard inverted microscope (Zeiss, Axiovert 200M) and the hydrodynamic geometry is defined by two reservoirs connected by a 300 µm long and 20 µm x 20 µm wide squared constriction (Figure 1a). A syringe pump (NemeSys, Cetoni) is used to drive a cell suspension through the narrow channel where cells are being deformed by hydrodynamic interaction only. Utilizing a combination of pressure and shear stress gradients individual cells are firstly elongated before relaxing into a parachute-like shape at the

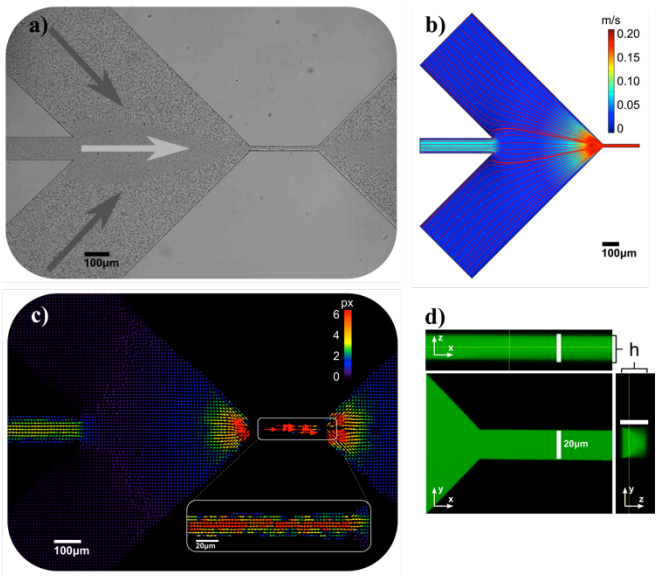

Figure 2: Characterization of microfluidic chip. a) Particle image velocimetry (PIV) of 1 µm polystyrene beads suspended in water. The total flow rate inside the channel is of 0.04 µl/s and is composed from the sheath flow (indicated by black arrows) and a central flow (indicated by white arrow). The length of the channel is 300 µm and the ratio between sheath flow and central flow is 3:1. b) Three dimensional finite element simulation of the experiment shown in a) indicating an expected maximal flow velocity of 0.2 m/s inside the channel. c) PIV analysis of two subsequent frames captured at 8,000 fps and revealing a bead velocity of 6 pixels ≈ 0.16 m/s. d) Reconstruction of chip geometry based on fluorescent staining and confocal microscopy.

rear part of the channel [25]. In this region of interest (ROI) a high-speed camera (MC1362, Mikrotron) captures images at 2,000 frames per second (fps) and the deformation of the cells is being detected and quantified based on a custom-built algorithm [20]. This can be summarized as follows (Figure 1b). After background subtraction a pixel thresholding step defines the presence of a cell within the ROI and the projected area A and perimeter l are determined by a contour following algorithm [26]. The deformation D is quantified by the circularity c:

$$D = 1 - c = 1 - \frac{2\sqrt{\pi A}}{l} \quad . \qquad (1)$$

The entire processing time for a single frame is less than 500 µs. Figure 1c shows an exemplary RT-DC plot of N=1,118 cells. As all data analyses are done in real-time an excess of 100 cells per second can be processed while measurement time is mainly limited by sample size.

Characterization of RT-DC

Cell mechanical characterization for RT-DC experiments is based on an analytical model [25] that relies on a laminar fluid flow inside the narrow channel. Hydrodynamics can be visualized using particle image velocimetry (PIV) where small beads in a moving fluid are observed. Here, 1 µm polystyrene beads (PS) at a concentration of 10^7 per ml have been suspended in water and pumped through a sheath flow microfluidic chip at a total flow rate of 0.04 µl/s (Figure 2a). Comparable to a glass cuvette in a flow cytometer the sheath flow is used to laterally align the cells inside the constriction zone. From full numerical simulations (Comsol) and utilizing the complete geometry in 3D we compute a maximum flow

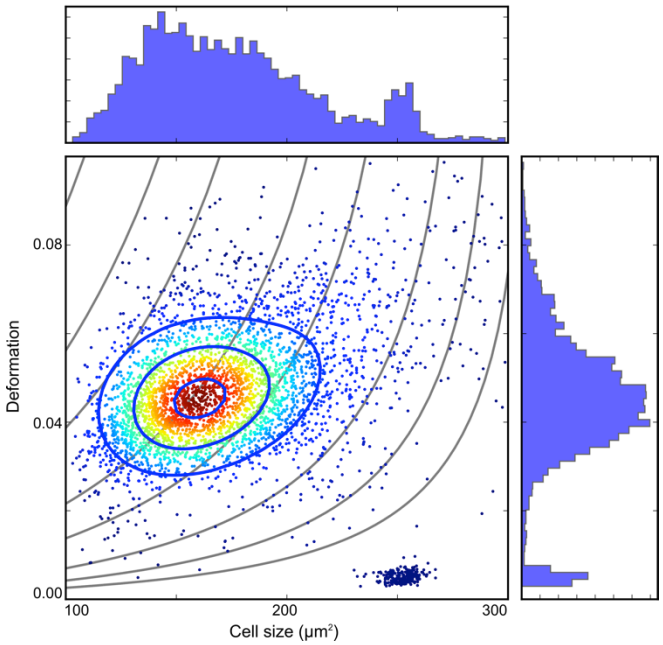

Figure 3: Identification of objects based on size and deformation. RT-DC plot of a heterogeneous mixture of 5% (v/v) (17.23 ± 0.24) µm diameter PMMA beads and HL60 cells adjusted to a concentration of $4 \cdot 10^6$ objects per ml. While the monodisperse beads are localized at the bottom right of the graph the cells form a heterogeneous population in the center of the plot indicating the finite deformation. Total number of objects *N*=4,958. Flow rate is 0.04 µl/s and a channel of 20 µm x 20 µm is used. 1d projection of measured quantities indicates a clear separation in cell size and deformation. The contour lines represent 90%, 50% and 20% of the maximum density, respectively.

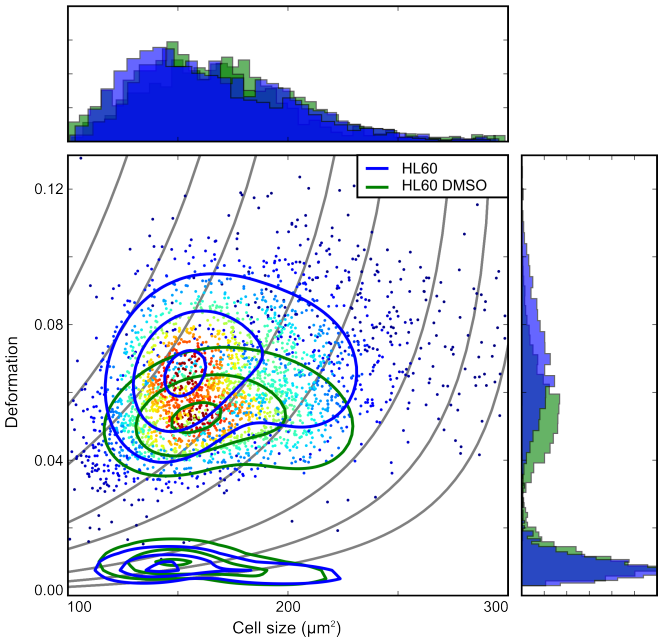

Figure 4: Effect of DMSO on cell deformation.. Alterations in HL60 cells after 10 minutes incubation using 10% dimethylsulfoxide (DMSO) and comparison to a control sample. DMSO-treated cells (*N*=2,445, green contour line) deform less compared to untreated cells (*N*=2,075, blue contour line) while the reference measurement in the reservoir (inset) reveals no difference. Measurements were carried out in a 20 µm x 20 µm channel at a flow rate of 0.08 µl/s. The contour lines represent 90%, 50% and 20% of the maximum density, respectively.

velocity of approximately 0.2 m/s (Figure 2b). Of note, assuming a circular cross-section having an equivalent channel radius [25] of 10 µm and applying the equations for Poiseuille flow results in a flow velocity of 0.25 m/s.

PIV is based on particle tracing and displacement vector calculation from cross-correlation of two subsequent frames within a time series. Here, images have been acquired at a frame rate of 8,000 fps and stored into video files. PIV analysis was performed using ImageJ (Wayne Rasband, NIH) resulting in a maximal bead displacement of 6 pixels between two subsequent frames. The resulting velocity of 0.16 m/s is close to the expected value from analytical and numerical calculations (Figure 2c). As this result agrees very well with both computational assays the flow can assumed to be laminar.

The cross-section of the channel was analyzed using confocal microscopy. The microfluidic chip was filled with 5 µM Alexa 488 (Sigma Aldrich) and an image stack was acquired using a LSM700 confocal microscope (Zeiss). Image reconstruction and visualization was performed using ImageJ. The projections in the *xy*-, *xz*- and *yz*-plane reveal a cross-section of 20 µm x 20 µm within the optical resolution of the microscope (Figure 2d).

Discrimination between beads and cells

RT-DC allows for the discrimination of objects based on size and deformation. Following the protocol highlighted in the Material and Methods section $4 \cdot 10^6$ HL60 cells were re-suspended in 1 ml of 0.5% (w/v) methyl cellulose and PBS-(MC-PBS). Afterwards PMMA beads of d=(17.23 ± 0.24) µm diameter (Microparticles) were added at a concentration of 5% (v/v). The resulting RT-DC plot for a constant flow rate of 0.04 µl/s is shown in Figure 3 and reveals two distinct populations. The monodisperse beads are localized in a very narrow spot at the bottom right of the graph having a mean object size of (252 ± 6) µm^2 (Gaussian fit to data of 1d projection, Figure 3 top). Assuming a circular cross-section of the beads the diameter can be calculated to 17.9 µm, which is within pixel accuracy to the manufactures value. As expected from beads made of PMMA the spheres do not deform at all showing a deformation close to 0. This is also confirmed by analyzing the 1d projection of the deformation values (Figure 3 right).

In contrast, the HL60 cells are represented by a heterogeneous population in the center of the scatter plot where the mean area is calculated to (162 ± 35) µm^2 while the mean deformation is (0.045 ± 0.01). Our algorithm allows for the determination of the number concentration of any sub-population. Here, the amount of PMMA beads measured is *N*=247 from a total number of *N*=4,958 objects. This equals a concentration of app. 5% which is in agreement with the initial value of the suspension of 5%. In conclusion, RT-DC allows not only for the discrimination of objects based on size and deformation but also for the identification of the concentration of each sub-population.

Effect of DMSO

The direct benefit of a label-free method for cell characterization is found in the identification of the biological state of a cell population. We demonstrate that RT-DC can be applied to track the effect of dimethylsulfoxide (DMSO) on cells, which is e.g. of high-relevance for drug-screening

assays or cryconservation of cells and tissues. As a proof-of-principle HL60 cells have been treated with 10% DMSO. DMSO penetrates cell membranes and causes ruptures at higher concentration and induces apoptosis and necrosis [21, 23].

Figure 4 compares HL60 cells after 10 minutes of incubation with DMSO (green contour line) to a control sample (blue contour line) in two separate experiments. As described above cells have been re-suspended in 0.5% MC-PBS to a final concentration of $2 \cdot 10^6$ per ml before being analysed in a 20 µm x 20 µm channel for each sample. Prior to mechanical characterization induction of apoptosis and necrosis was confirmed using a flow cytometer assay (FITC Annexin V / Dead Cell Apoptosis Kit, Invitrogen Molecular Probes, data not shown). While being similar in cell size Figure 4 reveals a distinct difference in deformation for both populations. DMSO treated cells deform less compared to the control sample while the reference measurement inside the reservoir (no mechanical stress, Figure 4 bottom) shows no differences. Therefore, RT-DC can be used to track the viability of cells.

IV. Conclusion

In summary, we have a demonstrated the ability of real-time deformability cytometry for label-free identification of PMMA beads and HL60 cells in heterogeneous samples. While colloids show no deformation, cells clearly respond to the hydrodynamic stress inside the microfluidic channel by a shape change that depends on their biological state. We utilize that knowledge by comparing cells before and after treatment with DMSO and find that apoptotic and necrotic cells deform less. This highlights, that RT-DC can in future also be incorporated into flow cytometer, so that mechanical cell characterization will find its way into standard fields of biological research.

Acknowledgment

The authors would like to thank Anna Taubenberger, Cornelia Liebers, Claudia Moex and Francois Amblard for technical support, advice and engaging discussions. Financial support from the Alexander-von-Humboldt Stiftung (Humboldt-Professorship to J. G.), the Sächsische Ministerium für Wissenschaft und Kunst (TG70 grant to O. O and J. G), the DFG-Center for Regenerative Medicine of the TU Dresden (seed grant to J. G.), the Deutsche Forschungsgemeinschaft (Gerok position to N. T.), the Deutsche Gesellschaft für Pädiatrische Infektiologie (N. T.) and the Studienstiftung des Deutschen Volkes (A. M.) and the Max-Planck Society (E. F. F.), is gratefully acknowledged.

References

[1] W. Pfeffer, “Osmotische Untersuchungen. Studien zur Zellmechanik.”, 1st ed. (Wilhelm Engelmann, Leipzig, 1877).

[2] A. E. Pelling and M. A. Horton, “A historical perspective on cell mechanics,” Pflugers Arch. (2008).

[3] K. E. Kasza, A. C. Rowat, J. Liu et al., “The cell as a material,” Curr. Opin. Cell Biol. 19 (1), 101 (2007).

[4] D. A. Fletcher and R. D. Mullins, “Cell mechanics and the cytoskeleton,” Nature 463 (7280), 485 (2010).

[5] E. L. Elson, “Cellular Mechanics as an indicator of cytoskeletal structure and function,” Annu. Rev. Biophys. Biophys. Chem. 17, 397 (1988).

[6] I. Titushkin and M. Cho, “Modulation of Cellular Mechanics during Osteogenic Differentiation of Human Mesenchymal Stem Cells,” Biophys. J. 93, 3693 (2007).

[7] F. Lautenschläger, S. Paschke, S. Schinkinger et al., “The regulatory role of cell mechanics for migration of differentiating myeloid cells,” Proc. Natl. Acad. Sci. U. S. A. 106 (37), 15696 (2009).

[8] C. L. Keefer and J. P. Desai, “Mechanical phenotyping of stem cells,” Theriogenology 75 (8), 1426 (2011).

[9] A. E. Ekpenyong, G. Whyte, K. Chalut et al., “Viscoelastic Properties of Differentiating Blood Cells are Fate- and Function-Dependent,” PLoS One 7 (9), e45237 (2012).

[10] O. Thoumine and A. Ott, “Comparison of the mechanical properties of normal and transformed fibroblasts,“ Biorheology 34 (4-5), 309 (1997).

[11] 11. M. Lekka, P. Laidler, D. Gil et al., “Elasticity of normal and cancerous human bladder cells studied by scanning force microscopy,“ Eur. Biophys. J. 28 (4), 312 (1999).

[12] J. Guck, S. Schinkinger, B. Lincoln et al., “Optical Deformability as an Inherent Cell Marker for Testing Malignant Transformation and Metastatic Competence,” Biophys. J. 88 (5), 3689 (2005).

[13] S. Suresh, “Biomechanics and biophysics of cancer cell,” Acta Biomater. 3 (4), 413 (2007).

[14] T. W. Remmerbach, F. Wottawah, J. Dietrich et al., “Oral Cancer Diagnosis by Mechanical Phenotyping,” Cancer Res. 69 (5), 1728 (2009).

[15] S. Kumar and V. M. Weaver, “Mechanics, malignancy, and metastasis: The force journey of a tumor cell,” Cancer Metastasis Rev. 28 (1-2), 113 (2009).

[16] H. T. Tse, D. R. Gossett, Y. S. Moon et al., “Quantitative Diagnosis of Malignant Pleural Effusions by Single-Cell Mechanophenotyping,” Sci. Transl. Med. 5 (212), 212ra163 (2013).

[17] K. J. Van Vliet, G. Bao, and S. Suresh, “The biomechanics toolbox: experimental approaches for living cells and biomolecules,” Acta Materialia 51, 5881 (2003).

[18] B. D. Hoffman and J. C. Crocker, “Cell Mechanics: Dissecting the Physical Responses of Cells to Force,” Annu. Rev. Biomed. Eng. 11 (1), 259 (2009).

[19] D. R. Gossett, H. T. Tse, S. A. Lee et al., “Hydrodynamic stretching of single cells for large population mechanical phenotyping,” Proc. Natl. Acad. Sci. U. S. A. 109 (20), 7630 (2012).

[20] O. Otto, P. Rosendahl, A. Mietke et al., “Real-time deformability cytometry: on-the-fly cell mechanical phenotyping,” Nat. Methods 12(3), 199 - 202 (2015)

[21] N. C. Santos, J. Figueira-Coelho, J. Martins-Silva, and C. Saldanha, “Multidisciplinary utilization of dimethyl sulfoxide: pharmacological, cellular, and molecular aspects,” Biochem. Pharmacol. 65, 1035 – 1041 (2003)

[22] S. Golfier, “Cell mechanics on millisecond timescales in microfluidic system,” Diploma Thesis (2014)

[23] R. Pal, M. K. Mamidi, A. K. Das, and R. Bhonde, “Diverse effects of dimethyl sulfoxide (DMSO) on the differentiation potential of human embryonic stem cells,” Arch. Toxicol. 86, 651 – 661 (2012)

[24] J. Liu, H. Yoshikawa, Y. Nakajima, and K. Tasaka, “Involvement of mitochondrial permeability transition and caspase-9 activation in dimethyl sulfoxide-induced apoptosis of EL-9 lymphoma cells,” Int. Immunopharmacol. 1, 63 – 74 (2001)

[25] A. Mietke, O. Otto, S. Girardo et al., “Extracting cell stiffness from real-time deformability cytometry – a theoretical and experimental study,” submitted for publication

[26] S. Suzuki, and K, Abe, “Topological Structural Analysis of Digital Binary Images by Border Following,“ Comput. Vis. Graph. Image Process. 30, 32-46 (1985)